Biogeosciences Discuss., doi:10.5194/bg-2017-43, 2017
Manuscript under review for journal Biogeosciences
Discussion started: 22 February 2017

Biogeosciences Discussions Open Access EGU

Tracing the origin of the oxygen-consuming organic matter in the hypoxic zone in a large eutrophic estuary: the lower reach of the Pearl River Estuary, China

Jianzhong Su[1], Minhan Dai[1*], Biyan He[1, 2], Lifang Wang[1], Jianping Gan[3], Xianghui Guo[1], Huade Zhao[1] and Fengling Yu[1]

[1]State Key Laboratory of Marine Environmental Science, Xiamen University, Xiamen, China
[2]College of Food and Biological Engineering, Jimei University, Xiamen, China
[3]Department of Mathematics and Division of Environment, Hong Kong University of Science and Technology, Kowloon, Hong Kong, China

Correspondence to: Minhan Dai (mdai@xmu.edu.cn)

Abstract. We assess the relative contributions of differently sourced organic matter, marine vs. terrestrial, to oxygen consumption in an emerging hypoxic zone in the lower Pearl River Estuary (PRE), a large eutrophic estuary located in Southern China. Our cruise, conducted in July 2014, contained two legs before and after a passing through of Typhoon Rammasun, which destroyed the water stratification. The stratification recovered rather quickly within one day after the typhoon. We observed, in both legs, algal blooms in the surface water with hypoxias underneath in the bottom water. The repeated samplings at the initial hypoxic station showed severe oxygen depletion down to 30.3 μmol kg^{-1} before the typhoon and a clear drawdown of dissolved oxygen after the typhoon. Based on a three end-member mixing model and the mass balance of dissolved inorganic carbon and its isotopic composition, we derived the $\delta^{13}C$ of the remineralized organic carbon as -21.8±0.6 ‰ in the hypoxia. We estimated that 73±10 % of the oxygen-consuming organic matter was marine sourced and, the rest 27±10 % was terrestrially sourced. Contrasting to the hypoxic site in the East China Sea off the Changjiang Estuary where eutrophication-stimulated marine sourced organic matter prevailed the oxygen consumption, the terrestrially sourced organic matter significantly contributed to the formation and maintenance of the hypoxia in the present study site. The difference in oxygen sinks in different systems has important implications in better understanding to the controls of hypoxias and their mitigations.

Biogeosciences Discuss., doi:10.5194/bg-2017-43, 2017
Manuscript under review for journal Biogeosciences
Discussion started: 22 February 2017

1 Introduction

The occurrence of hypoxias has been exacerbated worldwide (Nixon, 1995; Rabalais et al., 2010; Zhang et al., 2013). In recent decades, more than 400 coastal hypoxic systems are reported with an exponential growth rate of 5.5±0.23 % yr^{-1}, demonstrating the persistence and complexity in both science and management (Vaquer-Sunyer and Duarte, 2008; Diaz and Rosenberg, 2008). Hypoxia may not only reduce the biodiversity, endanger aquatic and benthic habitats, but also alter the redox chemistry in both the water column and the underlying sediments, triggering secondary pollutants in the water body (Breitburg, 2002; Rutger et al., 2002). Moreover, the hysteresis-like behavior involved in the recovery from hypoxia, due to the differential timescales of biological loss (within hours to weeks) and recovery from hypoxia (from months to years), indicates the difficulties in the restoring process and urgency for proper managerial actions (Steckbauer et al., 2011).

Coastal hypoxia usually occur to stratified water columns where the downward mixing of oxygen from the surface is impeded (Kemp et al., 2009). Below the pycnocline, the aerobic respiratory process is usually the predominant sink of oxygen. Organic matter that consumes dissolved oxygen (DO) is thus the ultimate cause of hypoxia under favourable physical settings (Rabouille et al., 2008; Rabalais et al., 2014; Qian et al., 2016a). The organic carbon (OC) that fuels the respiratory reduction of oxygen could originate from the eutrophication-induced primary production (marine sourced OC, OC_{mar}) and terrestrially natural leaching and anthropogenic drainage (terrestrially sourced OC, OC_{terr}) (Paerl, 2006; Rabalais et al., 2010).

The question of how much OC in the bottom hypoxic zone is imported from the on-site primary production versus how much OC is derived from terrestrial sources has been an issue of debate (Wang et al., 2016). Much of the phytoplankton-centric hypoxia literature suggests that the OC_{mar} dominates the oxygen consumption in hypoxic zones owing to the higher microbial availability (Zimmerman and Canuel, 2000; Boesch et al., 2009; Carstensen et al., 2014). Wang et al. (2016) quantified for the first time the relative contributions of particulate OC_{mar} (POC_{mar}) and particulate OC_{terr} (POC_{terr}) in consuming DO in the bottom water of the East China Sea (ECS) off the Changjiang Estuary (CJE), and found that POC_{mar} prevailed in DO consumption. There existed other studies showing that terrestrially sourced organic matter may also be important (Swarzenski et al., 2008; Bianchi, 2011a; Bianchi et al.,

Biogeosciences Discuss., doi:10.5194/bg-2017-43, 2017
Manuscript under review for journal Biogeosciences
Discussion started: 22 February 2017

2011b). It is thus highly significant to quantify the relative contributions of organic matter (OC_{mar} vs. OC_{terr}) in different systems, since reducing organic matter and nutrient loadings would require different management strategies.

The Pearl River Estuary (PRE, 21.2 ° N–23.1 ° N, 113.0 ° E–114.5 ° E) is surrounded by large cities including Hong Kong, Shenzhen and Guangzhou and has received very high loads of nutrients from the drainage basin in the last three decades, and eutrophication has increasingly become an issue of concern (Ye et al., 2012; Huang et al., 2003). The dissolved inorganic nitrogen concentration in the PRE has increased about 4-fold in 2002 (76.1 μmol L^{-1}) compared with 1986 (19.3 μmol L^{-1}) (He and Yuan, 2007). Such an increase arises mainly from the intensifying domestic sewage, industrial wastewater, agricultural runoff and aquaculture in the watershed (Huang et al., 2003).

Recent observations by Qian et al. (Submitted) based on their monthly surveys between April 2010 and March 2011 together with the long term monitoring data from 1990 to 2014 have suggested that the lower PRE has emerged as a seasonal hypoxic zone (Qian et al., 2016b). Moreover, during our cruise, two relatively large hypoxic zones (~1000 km^2) occurred in the lower PRE with DO <3 mg L^{-1}. However, the origin of the organic matter that induced the emerging hypoxia in the lower PRE has not been examined. The present study thus sought to assess in a quantitative way the origin of the oxygen-consuming organic matter in the lower PRE, an economically important region. We point out that such a study has additionally significant societal relevance, such as the water quality in the vicinityof Hong Kong located at the lower PRE. The government of Hong Kong is examining the efficacy of its costly Harbour Area Treatment Scheme project and if additional treatment should be implemented (http://www.gov.hk/en/residents/environment/water/harbourarea.htm).

2 Materials and Methods

2.1 Sampling and analysis

Interrupted by Typhoon Rammasun on 17-18 July 2014, our cruise was divided into two legs (Fig. 1). In Leg 1 on 13–16 July, we sampled Sections F4, F5 and Stations A08–A18. During Leg 2 on 19–27 July, we sampled Stations A01–A10, Sections F3, F4, Stations A11–A17 and Sections F5, F6, F1, F2 in

sequence. In order to monitor the development of the hypoxia before and after the typhoon event, we revisited Station A10 three more times (13, 20 and 27 July).

According to the gauge records in the upper Pearl River, water discharge peaked in June and July. Typhoon Rammasun brought about a relatively high discharge (26115 m^3 s^{-1}) on 16 July. Nevertheless, the freshwater discharge during our cruise was rather comparable to the long-term (2000–2011) monthly average, suggesting that this study represented a typical situation of the area in terms of terrestrial material discharge.

Temperature and salinity were determined with a SBE 25 Conductivity-Temperature-Depth/Pressure unit (Sea-Bird Co.). Water samples were collected using 4 L Go-Flo bottles (General Oceanics). The DO concentrations in discrete samples were measured on board using the classic Winkler procedure within 8 h (Dai et al., 2006). DIC was measured with an infrared detector after acidifying 0.5–0.7 mL of water sample with a precision of 0.1 % for estuarine and sea waters (Cai et al., 2004). Dissolved calcium concentration (Ca^{2+}) was determined using an EGTA titration with a Metrohm 809 TITRANDO potentiometer, which has a precision better than ± 5 μmol kg^{-1} (Cao et al., 2011).

For the analysis of $\delta^{13}C_{DIC}$, an ~20 mL DIC sample was converted into gaseous CO_2 and progressively purified through a vacuum line. The pure CO_2 sample was analyzed with an isotope ratio mass spectrometer (IRMS, Finnigan MAT 252, Bremen, Germany). The analytical precision was better than 0.1 ‰.

TSM (total suspended matter), POC and $\delta^{13}C_{POC}$ samples were concentrated onto a preweighed and pre-combusted 0.7 μm Whatman GF/F filters after filtering 0.2–1.0 L water under a mild vacuum (~ 25 kPa). Filters were washed with distilled water and stored under a -20 ℃ environment. Before analysis, the filters were freeze-dried. The TSM was determined using the net weight increment on the filter and the filtration volume. The filters were decarbonated with 1.0 mol L^{-1} HCl and dried at 40 ℃ for 48 h (Kao et al., 2012) and analyzed for POC and $\delta^{13}C_{POC}$ on an elemental analyzer coupled with an isotope-ratio mass spectrometer (IRMS). The analytical precision for $\delta^{13}C_{POC}$ was better than 0.1 ‰. Chl-a was measured using a Turner fluorometer after extraction of the filter samples with 90 % acetone (He et al., 2010b). Calibrations were performed using Sigma Chl-a standard.

Biogeosciences Discuss., doi:10.5194/bg-2017-43, 2017
Manuscript under review for journal Biogeosciences
Discussion started: 22 February 2017

2.2 Three end-member mixing model

We adopted a three end-member mixing model to construct the conservative mixing scheme among different water masses (Cao et al., 2011; Han et al., 2012):

$$F_{RI}+F_{SW}+F_{SUB}=1 \quad (1)$$

$$\theta_{RI}\times F_{RI}+\theta_{SW}\times F_{SW}+\theta_{SUB}\times F_{SUB}=\theta \quad (2)$$

$$S_{RI}\times F_{RI}+S_{SW}\times F_{SW}+S_{SUB}\times F_{SUB}=S \quad (3)$$

where θ and S represent the potential temperature and salinity; the subscripts RI, SW, SUB denote the three different water masses (the Pearl River plume water, the offshore surface seawater and the upwelled subsurface water); and F_{RI}, F_{SW}, F_{SUB} represent the fractions that each end-member contributes to the in situ samples. Then, these fractions were applied to predict the DIC and its isotopic composition ($\delta^{13}C_{DIC}$) solely from conservative mixing. The difference (Δ) between measurement and prediction values could be acquired, which represented the magnitude of the biological alteration (Wang et al., 2016).

3 Results

3.1 Horizontal distribution

The average freshwater discharge rate during our cruises (16369 $m^3 s^{-1}$) showed a minor difference (<5 %) with the multi-years (2000–2011) monthly mean discharge (15671 $m^3 s^{-1}$). We noted that the survey area in Leg 1 was smaller, covering only outside Lingdingyang Bay, traditionally regarded as PRE. While, in Leg 2, the survey area covered the Lingdingyang Bay from the Humen Outlet to the adjacent coastal sea.

In each leg, we found an algal bloom zone at the surface and a hypoxic zone at the bottom (Fig. 2). In Leg 1, the bloom zone, located to the east of the Wanshan Islands, was oxygen supersaturated with the highest DO saturation (DO%) greater than 160 % at Station F503, coupled with higher Chl-a (8.0 μg kg^{-1}) and lower surface DIC (1606.8 μmol kg^{-1}). Meanwhile, the bottom hypoxia lay more landward and the center's DO was as low as 30.3 μmol kg^{-1} at Station A10, along with higher DIC (2074.9 μmol kg^{-1}). However, in Leg 2, the bloom zone was more westward and larger than the former one, with the highest DO% greater than 140 % at Station A14. In spite of the disappearance of the previous hypoxia near

Biogeosciences Discuss., doi:10.5194/bg-2017-43, 2017
Manuscript under review for journal Biogeosciences
Discussion started: 22 February 2017

Station A10, another hypoxic zone was discovered to the southeast of the Wanshan Islands, with a lowest DO value of 7.2 μmol kg^{-1} and a higher DIC (2146.1 μmol kg^{-1}) in F304. We were unable to precisely constrain the areas of the bottom hypoxia due to the limited spatial coverage, but they covered at least ~900 km^2 and ~800 km^2 for Legs 1 and 2.

3.2 Vertical distribution

In Leg 1, the plume water reached 50 km away from the entrance of the PRE, and formed a 5–10 m thick plume (Fig. 3a–e). Both the thermocline and halocline contributed to the stability of the water structure, which favored the formation of the bottom hypoxia. The thickness of the bottom hypoxia was ~10 m. The algal bloom zone was not right above the hypoxia, but more seaward.

In Leg 2, although the typhoon attack would absorb enormous potential heat and aggravate water mixing, the enhanced freshwater discharge could soon make the stratification strong enough for the formation of hypoxia. At this time, the hypoxia was right below the bloom zone, with a thickness of 7 m (Fig. 3f–j). Also, near the Humen Outlet, we found low DIC (1466.3 μmol kg^{-1}) and moderately low DO water (89.1 μmol kg^{-1}), which reflected the input of the low DO water mass from the upstream as reported previously (Dai et al., 2006; Dai et al., 2008a; He et al., 2014).

3.3 Isotopic composition of DIC and POC

The $\delta^{13}C$ of DIC became heavier from freshwater (~ -11.4 ‰) to off-shore seawater (~ -0.6 ‰), with a relatively wide range beyond salinity=13 (Fig. 4). Owing to a malfunction of the machine, the $\delta^{13}C_{POC}$ data from our cruise were not available. Instead, we reported a valid $\delta^{13}C_{POC}$ dataset from a 2015 summer cruise in nearly the same region. The $\delta^{13}C$ of POC showed a similar trend with $\delta^{13}C_{DIC}$, i.e. ^{13}C enriched seaward, from ~ -28 ‰ to ~ -20 ‰. In the algal bloom zone, where the DO% was beyond 125 %, the mean $\delta^{13}C$ value for POC was -19.4±0.8 ‰ (n=8), which was within the typical range of the marine phytoplankton (Peterson and Fry, 1987). As shown in Fig. 4, there was a $\delta^{13}C_{POC}$ trough near a salinity of 15. Geologically, it was located at the mixing dominated zone in the inner Lingdingyang Bay, where intense resuspension of ^{13}C depleted sediment may occur (Guo et al., 2009).

Biogeosciences Discuss., doi:10.5194/bg-2017-43, 2017
Manuscript under review for journal Biogeosciences
Discussion started: 22 February 2017

3.4 Reinstatement of the hypoxic station after Typhoon Rammasun

Typhoon Rammasun landed on Zhanjiang located 400 km to the southwest of the PRE at 20:00 LT on 18 July and was dissipated at 05:00 LT on 20 July. This typhoon destroyed the water stratification. However, the associated heavy precipitation and rising runoff appeared to reestablish the stratification rather quickly, within one day, as suggested by the saline gradients (18–30) within the 0–10 m depth during our revisit at 15:20 LT on 20 July (Fig. 5b). In order to capture the evolution of oxygen between stratification disruption and reinstatement, we resumed our cruise and revisited Station A10 on 13, 20 and 27 July (Fig. 5). On 13 July, the bottom water of Station A10 was the hypoxic core, with the lowest DO (30.3 μmol kg^{-1}) and highest DIC (2074.9 μmol kg^{-1}). On 20 July, the results showed that the temperature homogeneous layer in the bottom water (9–13 m) might be the trail of the typhoon induced mixing (Fig. 5a), while the saline stratification (<9 m) depicted the rapid recuperation as a result of enhanced freshwater discharge (Fig. 5b). The bottom DO increased to 153.1 μmol kg^{-1} and the DIC decreased to 1900.7 μmol kg^{-1} because of the water mixing and aeration. In addition, the TSM increased sharply from 20.2 to 36.6 mg kg^{-1}, suggesting strong sediment resuspension. On 27 July, one week after the typhoon, the homogenous mixing layer in the bottom disappeared and strong thermohaline stratification occupied the whole water column again. Along with the intensifying stratification, the bottom DO decreased to 98.6 μmol kg^{-1} indicating continuous DO depletion and the potential trend for hypoxia formation. Meanwhile, the bottom DIC increased to 2000.1 μmol kg^{-1} and the dissolved inorganic phosphate (DIP) rose from 0.28 to 0.57 μmol kg^{-1}. Moreover, the bottom-water TSM returned to the same level as prior to the typhoon (13 July).

4 Discussion

4.1 Selection of end-members and model validation

The potential temperature-salinity plot displayed a three end-member mixing scheme over the PRE and the adjacent coastal water (Fig. 6a), consisting of the Pearl River plume water, offshore surface seawater and the upwelled subsurface water. In summer, the DIC was ~1917 μmol kg^{-1} at S=33.7, which can be regarded as the off-shore surface seawater end-member (Guo and Wong, 2015). When we chose S=34.6 as the off-shore subsurface water salinity end-member, we obtained a DIC of ~2023 μmol kg^{-1}. For the

Biogeosciences Discuss., doi:10.5194/bg-2017-43, 2017
Manuscript under review for journal Biogeosciences
Discussion started: 22 February 2017

plume end-member, it was difficult to directly select from the field data, because biological alteration within the plume influenced area might lead to an improper calculation result. Therefore, we first assumed that the plume water was the mixture between the freshwater water and off-shore surface seawater. Then, we compiled a 3 years' surface dataset in summer (August 2012, July 2014 and July 2015) to extrapolate the relatively stable freshwater end-member so as to examine the biological effect along with salinity. From the constraint of the DIC end-members (freshwater and off-shore surface seawater), we observed that DIC remained overall conservative when salinity was <10.8 but showed removal when salinity >10.8 (Han et al., 2012). Thus, we derived plume end-member values from the property-salinity conservative mixing curve at salinity=10.8. Furthermore, S=10.8 was located on the innermost station (A08) in Leg 1, which coincided with the spatial and temporal scale of the actual water mass mixing in our survey. As a guarantee, we also used a freshwater end-member (S=0), but the outputs of the model showed little difference from those based on the plume end-member at S=10.8. The summary of the end-member values in this study is listed in Table 1.

We calculated the water fractions of the three water parcels based on potential temperature and salinity equations, so as to predict DIC and its isotopic composition ($\delta^{13}C_{DIC}$) solely from conservative mixing. We chose the concentration of Ca^{2+} as a conservative tracer to validate our model prediction, and the model derived values were in good accordance with the field-observed values (Fig. 6b), which strongly supported our model prediction.

As shown in Fig. 6c, most of the observed DIC in the subsurface water was higher than the predicted values, as a result of the DIC production via OC oxidation. On the other hand, the majority of observed $\delta^{13}C_{DIC}$ values became lighter than the predicted ones, owing to the accumulation of lighter carbon remineralized from the organic matter (Fig. 6d). Based on the difference between the observed and predicted values of DIC and $\delta^{13}C_{DIC}$, the carbon isotopic composition of the oxygen-consuming organic matter could be traced precisely (see details in Sect. 4.2).

In the subsurface water, most of the ΔDIC varied from 0 to 132.3 μmol kg^{-1}, coupled with an apparent oxygen utilization (AOU) increment from 0 to 179.1 μmol kg^{-1}. ΔDIC had a positive correlation with the AOU (Fig. 6e), corresponding with the fact that the additional DIC was primarily produced by organic matter remineralization via aerobic respiration. The slope of ΔDIC vs. AOU in the subsurface water was

Biogeosciences Discuss., doi:10.5194/bg-2017-43, 2017
Manuscript under review for journal Biogeosciences
Discussion started: 22 February 2017

0.75±0.03, which matched well with the classic Redfield stoichiometry (i.e., 106/138=0.77), providing further evidence for the occurrence of aerobic respiration.

4.2 Isotopic composition of the oxygen-consuming OC

The mass balance of DIC isotopic composition is shown by Eq. (4) (Wang et al., 2016):

$$\delta^{13}C_{DICobs} \times DIC_{obs} = \delta^{13}C_{DICpre} \times DIC_{pre} + \delta^{13}C_{DICbio} \times DIC_{bio} \quad (4)$$

where the subscripts obs, pre and bio refer to the field-observed, model-predicted and biologically altered values.

Degradation of OC generally produces DIC with minor isotopic fractionation relative to the OC substrate (Hullar et al., 1996; Breteler et al., 2002). Thus, the isotopic composition of DIC_{bio} (i.e., $\delta^{13}C_{DICbio}$) should be identical to the $\delta^{13}C_{OCx}$ of the OC, which consumed oxygen and produced DIC_{bio}, and the $\delta^{13}C_{OCx}$ could be derived from the mass balance equations of both DIC and its stable isotope:

$$\delta^{13}C_{OCx} = \frac{\delta^{13}C_{obs} \times DIC_{obs} - \delta^{13}C_{pre} \times DIC_{pre}}{DIC_{obs} - DIC_{pre}} \quad (5)$$

Equation (5) can be rearranged into Eq. (6):

$$\Delta(\delta^{13}C_{DIC} \times DIC) = \delta^{13}C_{OCx} \times \Delta DIC \quad (6)$$

As shown in Fig. 7, the slope of the linear regression represents $\delta^{13}C_{OCx}$ or $\delta^{13}C_{DICbio}$, which equals -21.8±0.6 ‰, reflecting a general $\delta^{13}C$ of the remineralized organic matter (Wang et al., 2016). The average $\delta^{13}C$ of POC samples near the Humen Outlet (S<4) was -28.3±0.7 ‰ (n=7), representing terrestrial origin. Previous studies adopt the $\delta^{13}C$ values of the terrigenous OC end-member in the PRE from -28.7 to -24.9 ‰ (He et al., 2010a; Yu et al., 2010; Hu et al., 2006). Likewise, Yu et al. (2010) report that the terrigenous freshwater POC has $\delta^{13}C$ around -28.7 ‰, reflecting a mixed nature of the C3 plant fragments and forest soils. For the surface water data (n=8) at stations with high salinity (S>26) and high DO saturation (DO%>125 %), the average $\delta^{13}C_{POC}$ value was -19.4±0.8 ‰, reflecting a stable carbon isotopic signature mainly from the marine phytoplankton biomass. Since previous studies choose a marine OC end-member from -21.2 to -20.5 ‰ (He et al., 2010a; Yu et al., 2010; Hu et al., 2006; Chen et al., 2008), it was reasonable to assign -19.4±0.8 ‰ as the $\delta^{13}C$ value of OC_{mar} in the PRE and the adjacent coastal water.

Biogeosciences Discuss., doi:10.5194/bg-2017-43, 2017
Manuscript under review for journal Biogeosciences
Discussion started: 22 February 2017

Although studies have shown the effects of selective diagenesis of organic matter fractions that are isotopically heavy or light (Marthur et al., 1992; Lehmann et al., 2002), these effects are small compared to the isotopic differences among differently sourced organic matter (Meyers, 1997). It is thus reasonable to assume that the isotopic ratios are conservative and that the end-member sources determine the isotopic distributions of organic matter in natural systems (Cifuentes et al., 1988). The relative contributions from marine and terrestrially sourced organic matter to oxygen-consuming organic matter could be estimated based on the following equation (Shultz and Calder, 1976; Hu et al., 2006):

$$f(\%) = \frac{\delta^{13}C_{mar} - \delta^{13}C_{OCx}}{\delta^{13}C_{mar} - \delta^{13}C_{terr}} \times 100 \quad (7)$$

The result showed that the marine sourced organic matter contributed 73±10 % to the oxygen-consuming organic matter pool, while the terrestrially sourced organic matter accounted for the remaining 27±10 %. It is thus clear that the marine organic matter from eutrophication-induced primary production dominated oxygen consumption in the hypoxic zone while the terrestrially sourced organic matter also significantly contributed to the formation and maintenance of hypoxia in the lower PRE and the adjacent coastal water.

The processes involved in the source partitioning of organic matter, their isotopic signals and their subsequent biogeochemical processes in the hypoxic zone are illustrated in the conceptual diagram in Fig. 8. River delivers a significant amount of nutrients and terrestrial organic matter into the estuary, stimulating phytoplankton blooms in the surface water at the lower reach of the estuary where turbidity is relatively low and conditions are favorable for phytoplankton growth (Gaston et al., 2006; Dai et al., 2008b; Guo et al., 2009). The subsequent sinking of the biomasses and the delivered terrestrial organic matter below the pycnocline consume oxygen and add respired DIC into subsurface water, thereby forming a coastal hypoxia. Within the hypoxic zone, the most important biological process is aerobic respiration.

As one of the largest rivers in the world, the Changjiang has been suffering from eutrophication for the past few decades (Zhang et al., 1999; Wang et al., 2014). In summer, sharp density gradients with frequent algal blooms and subsequent organic matter decomposition cause seasonal hypoxia in the bottom water of the ECS off the CJE. Wang *et al* (2016) revealed that the remineralization of marine sourced organic matter, OC_{mar}, overwhelmingly (nearly 100 %) contributed to DO consumption in the

ECS off the CJE. However, our present study showed that less OC_{mar} contributed to the oxygen depletion (73±10 %) in the hypoxic zone of the lower PRE. The exact reasons causing such a difference between two systems are unclear. However, it might be related to the differences in the bioavailability of OC_{terr}, microbial community and physical settings between these two hypoxic systems. First of all, although C3 plants dominate and C4 plants are minor in both the Pearl River and Changjiang drainage basins (Hu et al., 2006; Zhu et al., 2011), the OC_{terr} has gone through different extent of degradation within the estuaries before being transported into the hypoxic zones. In the CJE, approximate 50 % of the OC_{terr} has been mineralized down the estuary likely due to efficient OM unloading from mineral surfaces (Zhu et al., 2011). On the contrary, the PRE appears to be a somewhat intermediate site with respect to the export of OC_{terr}, being closely associated with sedimentary regimes and not characterized by extensive degradative loss (Strong et al., 2012). Thus, the bioavailability of OC_{terr} is likely higher in the PRE than in the CJE. Secondly, the difference in bacterial community structure between two systems may also play a role. Recent studies have demonstrated that the bacterial community was characterized by higher relative abundances of Actinobacteria and lower relative abundances of Cytophaga-Flavobacteria-Bacteroides (CFB) in the PRE than in the CJE (Zhang et al., 2016; Liu et al., 2012). Whether such differences would promote the degradation of OC_{terr} in the PRE remains to be known. Finally, the temperature of the bottom water in the PRE hypoxia (27–29 ℃) was higher than in the CJE hypoxia (21.5–24.0 ℃), which may have accelerated the rates of bacterial decomposition and growth (Brown et al., 2004).

5 Conclusions

Based on a three end-member mixing model and the mass balance of dissolved inorganic carbon and its isotopic composition, we demonstrated that the decomposed organic matter via aerobic respiration consisted of a major portion of OC_{mar} (73±10 %) and a less but significant portion of OC_{terr} (27±10 %), in the stratified subsurface waters of the lower PRE and the adjacent coastal water. Such source partitioning of organic matter in oxygen sinks differed from the hypoxic zone off the CJE. The difference in oxygen sinks in different systems has important implications in better understanding to the controls of hypoxias and their mitigations. Nevertheless, corresponding to the increasing nutrient levels, a significant implication of the present study is that reducing and managing nutrients is critical to control

eutrophication and to subsequently mitigate hypoxias (Conley et al., 2009; Paerl, 2009; Stefan et al., 2016; Mercedes et al., 2015). Given the fact that, the terrestrially sourced organic carbon also contributed to the consumption of oxygen in the lower PRE hypoxic zone, it is also crucial to characterize these oxygen-consuming terrestrial organic matter from natural soil leaching and/or anthropogenic wastewater discharge so as to make proper policies for hypoxia remediation.

*Acknowledgments***.** This research was funded by the National Natural Science Foundation of China through grants 41130857, 41576085 and 41361164001. We thank Tengxiang Xie, Li Ma, Shengyao Sun, Chenhe Zheng and Liangrong Zou for their assistance in sample collections; Yan Li and Yawen Wei for providing the calcium concentration data; Liguo Guo, Tao Huang and Dawei Li for assisting on the measurements of DIC, nutrients and $\delta^{13}C_{POC}$. The captain and the crew of R/V *Kediao 8* are acknowledged for their cooperation during the cruise. Professor John Hodgkiss is thanked for his assistance with English.

References

Bianchi, T. S.: The role of terrestrially derived organic carbon in the coastal ocean: A changing paradigm and the priming effect, Proc. Natl. Acad. Sci. U.S.A., 108, 19473-19481, doi:10.1073/pnas.1017982108, 2011a.

Bianchi, T. S., Wysocki, L. A., Schreiner, K. M., Filley, T. R., Corbett, D. R., and Kolker, A. S.: Sources of terrestrial organic carbon in the Mississippi plume region: evidence for the importance of coastal marsh inputs, Aquat. Geochem., 17, 431-456, doi:10.1007/s10498-010-9110-3, 2011b.

Boesch, D. F., Boynton, W. R., Crowder, L. B., Diaz, R. J., Howarth, R. W., Mee, L. D., Nixon, S. W., Rabalais, N. N., Rosenberg, R., Sanders, J. G., Scavia, D., and Turner, R. E.: Nutrient Enrichment Drives Gulf of Mexico Hypoxia, Eos, Trans. Amer. Geophys. Union, 90, 117-118, doi:10.1029/2009EO140001, 2009.

Breitburg, D.: Effects of hypoxia, and the balance between hypoxia and enrichment, on coastal fishes and fisheries, Estuaries, 25, 767-781, doi:10.1007/BF02804904, 2002.

Breteler, W. C. K., Grice, K., Schouten, S., Kloosterhuis, H. T., and Damsté, J. S. S.: Stable carbon isotope fractionation in the marine copepod Temora longicornis: unexpectedly low $\delta^{13}C$ value of faecal pellets, Mar. Ecol. Prog. Ser., 240, 195-204, doi:10.3354/meps240195, 2002.

Brown, J. H., Gillooly, J. F., Allen, A. P., Savage, V. M., and West, G. B.: Toward a metabolic theory of ecology, Ecology, 85, 1771-1789, doi:10.1890/03-9000, 2004.

Cai, W.-J., Dai, M., Wang, Y., Zhai, W., Huang, T., Chen, S., Zhang, F., Chen, Z., and Wang, Z.: The biogeochemistry of inorganic carbon and nutrients in the Pearl River estuary and the adjacent Northern South China Sea, Cont. Shelf Res., 24, 1301-1319, doi:10.1016/j.csr.2004.04.005, 2004.

Cao, Z., Dai, M., Zheng, N., Wang, D., Li, Q., Zhai, W., Meng, F., and Gan, J.: Dynamics of the carbonate system in a large continental shelf system under the influence of both a river plume and coastal upwelling, J. Geophys. Res. Biogeosci., 116, G02010, doi:10.1029/2010JG001596, 2011.

Carstensen, J., Andersen, J. H., Gustafsson, B. G., and Conley, D. J.: Deoxygenation of the Baltic Sea during the last century, Proc. Natl. Acad. Sci. U.S.A., 111, 5628-5633, doi:10.1073/pnas.1323156111, 2014.

Chen, F., Zhang, L., Yang, Y., and Zhang, D.: Chemical and isotopic alteration of organic matter during early diagenesis: Evidence from the coastal area off-shore the Pearl River estuary, south China, J. Mar. Syst., 74, 372-380, doi:10.1016/j.jmarsys.2008.02.004, 2008.

Cifuentes, L., Sharp, J., and Fogel, M. L.: Stable carbon and nitrogen isotope biogeochemistry in the Delaware estuary, Limnol. Oceanogr., 33, 1102-1115, doi:10.4319/lo.1988.33.5.1102, 1988.

Conley, D. J., Paerl, H. W., Howarth, R. W., Boesch, D. F., Seitzinger, S. P., Karl, E., Karl, E., Lancelot, C., Gene, E., and Gene, E.: Controlling eutrophication: nitrogen and phosphorus, Science, 123, 1014-1015, doi:10.1126/science.1167755, 2009.

Dai, M., Guo, X., Zhai, W., Yuan, L., Wang, B., Wang, L., Cai, P., Tang, T., and Cai, W.-J.: Oxygen depletion in the upper reach of the Pearl River estuary during a winter drought, Mar. Chem., 102, 159-169, doi:10.1016/j.marchem.2005.09.020, 2006.

Dai, M., Wang, L., Guo, X., Zhai, W., Li, Q., He, B., and Kao, S.-J.: Nitrification and inorganic nitrogen distribution in a large perturbed river/estuarine system: the Pearl River Estuary, China, Biogeosciences, 5, 1227-1244, doi:10.5194/bg-5-1227-2008, 2008a.

Dai, M., Zhai, W., Cai, W.-J., Callahan, J., Huang, B., Shang, S., Huang, T., Li, X., Lu, Z., Chen, W., and Chen, Z.: Effects of an estuarine plume-associated bloom on the carbonate system in the lower reaches of the Pearl River estuary and the coastal zone of the northern South China Sea, Cont. Shelf Res., 28, 1416-1423, doi: 10.1016/j.csr.2007.04.018, 2008b.

Diaz, R. J. and Rosenberg, R.: Spreading dead zones and consequences for marine ecosystems, Science, 321, 926-929, doi:10.1126/science.1156401, 2008.

Gaston, T. F., Schlacher, T. A., and Connolly, R. M.: Flood discharges of a small river into open coastal waters: Plume traits and material fate, Estuar. Coast. Shelf Sci., 69, 4-9, doi:10.1016/j.ecss.2006.03.015, 2006.

Guo, X., Dai, M., Zhai, W., Cai, W.-J., and Chen, B.: CO_2 flux and seasonal variability in a large subtropical estuarine system, the Pearl River Estuary, China, J. Geophys. Res. Biogeosci., 114, G03013, doi:10.1029/2008JG000905, 2009.

Guo, X. and Wong, G. T.: Carbonate chemistry in the northern South China Sea shelf-sea in June 2010, Deep-Sea Res. II, 117, 119-130, doi:10.1016/j.dsr2.2015.02.024, 2015.

Han, A., Dai, M., Kao, S.-J., Gan, J., Li, Q., Wang, L., Zhai, W., and Wang, L.: Nutrient dynamics and biological consumption in a large continental shelf system under the influence of both a river plume and coastal upwelling, Limnol. Oceanogr., 57, 486-502, doi:10.4319/lo.2012.57.2.0486, 2012.

He, B., Dai, M., Huang, W., Liu, Q., Chen, H., and Xu, L.: Sources and accumulation of organic carbon in the Pearl River Estuary surface sediment as indicated by elemental, stable carbon isotopic, and carbohydrate compositions, Biogeosciences, 7, 3343-3362, doi:10.5194/bg-7-3343-2010, 2010a.

He, B., Dai, M., Zhai, W., Wang, L., Wang, K., Chen, J., Lin, J., Han, A., and Xu, Y.: Distribution, degradation and dynamics of dissolved organic carbon and its major compound classes in the Pearl River estuary, China, Mar. Chem., 119, 52-64, doi:10.1016/j.marchem.2009.12.006, 2010b.

He, B., Dai, M., Zhai, W., Guo, X., and Wang, L.: Hypoxia in the upper reaches of the Pearl River Estuary and its maintenance mechanisms: A synthesis based on multiple year observations during 2000–2008, Mar. Chem., 167, 13-24, doi:10.1016/j.marchem.2014.07.003, 2014.

He, G.-f. and Yuan, G.-m.: Assessment of the water quality by fuzzy mathematics for last 20 years in Zhujiang Estuary, Mar. Environ. Sci., 26, 53-57, 2007.

Hu, J., Peng, P. a., Jia, G., Mai, B., and Zhang, G.: Distribution and sources of organic carbon, nitrogen and their isotopes in sediments of the subtropical Pearl River estuary and adjacent shelf, Southern China, Mar. Chem., 98, 274-285, doi:10.1016/j.marchem.2005.03.008, 2006.

Huang, X., Huang, L., and Yue, W.: The characteristics of nutrients and eutrophication in the Pearl River estuary, South China, Mar. Pollut. Bull., 47, 30-36, doi:10.1016/S0025-326X(02)00474-5, 2003.

Hullar, M., Fry, B., Peterson, B., and Wright, R.: Microbial utilization of estuarine dissolved organic carbon: a stable isotope tracer approach tested by mass balance, Appl. Environ. Microbiol., 62, 2489-2493, 1996.

Kao, S.-J., Terence Yang, J.-Y., Liu, K.-K., Dai, M., Chou, W.-C., Lin, H.-L., and Ren, H.: Isotope constraints on particulate nitrogen source and dynamics in the upper water column of the oligotrophic South China Sea, Global Biogeochem. Cycles, 26, GB2033, doi:10.1029/2011GB004091, 2012.

Kemp, W., Testa, J., Conley, D., Gilbert, D., and Hagy, J.: Temporal responses of coastal hypoxia to nutrient loading and physical controls, Biogeosciences, 6, 2985-3008, doi:10.5194/bg-6-2985-2009, 2009.

Lehmann, M. F., Bernasconi, S. M., Barbieri, A., and McKenzie, J. A.: Preservation of organic matter and alteration of its carbon and nitrogen isotope composition during simulated and in situ early sedimentary diagenesis, Geochim. Cosmochim. Acta, 66, 3573-3584, doi:10.1016/S0016-7037(02)00968-7, 2002.

Liu, M., Xiao, T., Wu, Y., Zhou, F., Huang, H., Bao, S., and Zhang, W.: Temporal distribution of bacterial community structure in the Changjiang Estuary hypoxia area and the adjacent East China Sea, Environ. Res. Lett., 7, 025001, doi:10.1088/1748-9326/7/2/025001, 2012.

Marthur, J. M., Tyson, R. V., Thomson, J., and Mattey, D.: Early diagenesis of marine organic matter: Alteration of the carbon isotopic composition, Mar. Geol., 105, 51-61, doi:10.1016/0025-3227(92)90181-G, 1992.

Mercedes, M. C. B., Luiz Antonio, M., Tibisay, P., Rafael, R., Jean Pierre, H. B. O., Felipe Siqueira, P., Silvia Rafaela Machado, L., and Sorena, M.: Nitrogen management challenges in major watersheds of South America, Environ. Res. Lett., 10, 065007, doi:10.1088/1748-9326/10/6/065007, 2015.

Meyers, P. A.: Organic geochemical proxies of paleoceanographic, paleolimnologic, and paleoclimatic processes, Org. Geochem., 27, 213-250, doi:10.1016/S0146-6380(97)00049-1, 1997.

Nixon, S. W.: Coastal marine eutrophication: A definition, social causes, and future concerns, Ophelia, 41, 199-219, doi:10.1080/00785236.1995.10422044, 1995.

Paerl, H. W.: Assessing and managing nutrient-enhanced eutrophication in estuarine and coastal waters: Interactive effects of human and climatic perturbations, Ecol. Eng., 26, 40-54, doi:10.1016/j.ecoleng.2005.09.006, 2006.

Paerl, H. W.: Controlling Eutrophication along the Freshwater–Marine Continuum: Dual Nutrient (N and P) Reductions are Essential, Estuar. Coast., 32, 593-601, doi:10.1007/s12237-009-9158-8, 2009.

Peterson, B. J. and Fry, B.: Stable Isotopes in Ecosystem Studies, Annu. Rev. Ecol. Syst., 18, 293-320, 1987.

Qian, W., Dai, M., Xu, M., Kao, S.-j., Du, C., Liu, J., Wang, H., Guo, L., and Wang, L.: Non-local drivers of the summer hypoxia in the East China Sea off the Changjiang Estuary, Estuar. Coast. Shelf Sci., doi:10.1016/j.ecss.2016.08.032, 2016a.

Qian, W., Gan, J., Liu, J., He, B., Lu, Z., Guo, X., Wang, D., Guo, L., Huang, T., and Dai, M.: Current status of emerging hypoxia in a large eutrophic estuary: the lower reach of Pearl River estuary, China, Submitted to Limnol. Oceanogr., 2016b.

Rabalais, N., Cai, W.-J., Carstensen, J., Conley, D., Fry, B., Hu, X., Quiñones-Rivera, Z., Rosenberg, R., Slomp, C., Turner, E., Voss, M., Wissel, B., and Zhang, J.: Eutrophication-Driven Deoxygenation in the Coastal Ocean, Oceanography, 27, 172-183, doi:10.5670/oceanog.2014.21, 2014.

Rabalais, N. N., Díaz, R. J., Levin, L. A., Turner, R. E., Gilbert, D., and Zhang, J.: Dynamics and distribution of natural and human-caused hypoxia, Biogeosciences, 7, 585-619, doi:10.5194/bg-7-585-2010, 2010.

Rabouille, C., Conley, D. J., Dai, M. H., Cai, W. J., Chen, C. T. A., Lansard, B., Green, R., Yin, K., Harrison, P. J., Dagg, M., and McKee, B.: Comparison of hypoxia among four river-dominated ocean margins: The Changjiang (Yangtze), Mississippi, Pearl, and Rhône rivers, Cont. Shelf Res., 28, 1527-1537, doi:10.1016/j.csr.2008.01.020, 2008.

Rutger, R., Stefan, A., Birthe, H., Hans, C. N., and Karl, N.: Recovery of marine benthic habitats and fauna in a Swedish fjord following improved oxygen conditions, Mar. Ecol. Prog. Ser., 234, 43-53, doi:10.3354/meps234043, 2002.

Shultz, D. J. and Calder, J. A.: Organic carbon 13C/12C variations in estuarine sediments, Geochim. Cosmochim. Acta, 40, 381-385, doi:10.1016/0016-7037(76)90002-8, 1976.

Steckbauer, A., Duarte, C. M., Carstensen, J., Vaquer-Sunyer, R., and Conley, D. J.: Ecosystem impacts of hypoxia: thresholds of hypoxia and pathways to recovery, Environ. Res. Lett., 6, 025003, doi:10.1088/1748-9326/6/2/025003, 2011.

Stefan, R., Mateete, B., Clare, M. H., Nancy, K., Wilfried, W., Xiaoyuan, Y., Albert, B., and Mark, A. S.: Synthesis and review: Tackling the nitrogen management challenge: from global to local scales, Environ. Res. Lett., 11, 120205, doi:10.1088/1748-9326/11/12/120205, 2016.

Strong, D. J., Flecker, R., Valdes, P. J., Wilkinson, I. P., Rees, J. G., Zong, Y. Q., Lloyd, J. M., Garrett, E., and Pancost, R. D.: Organic matter distribution in the modern sediments of the Pearl River Estuary, Org. Geochem., 49, 68-82, doi:10.1016/j.orggeochem.2012.04.011, 2012.

Swarzenski, P., Campbell, P., Osterman, L., and Poore, R.: A 1000-year sediment record of recurring hypoxia off the Mississippi River: The potential role of terrestrially-derived organic matter inputs, Mar. Chem., 109, 130-142, doi:10.1016/j.marchem.2008.01.003, 2008.

Vaquer-Sunyer, R. and Duarte, C. M.: Thresholds of hypoxia for marine biodiversity, Proc. Natl. Acad. Sci. U.S.A., 105, 15452-15457, doi:10.1073/pnas.0803833105, 2008.

Wang, H., Dai, M., Liu, J., Kao, S.-J., Zhang, C., Cai, W.-J., Wang, G., Qian, W., Zhao, M., and Sun, Z.: Eutrophication-Driven Hypoxia in the East China Sea off the Changjiang Estuary, Environ. Sci. Technol., 50, 2255-2263, doi:10.1021/acs.est.5b06211, 2016.

Wang, Q., Koshikawa, H., Liu, C., and Otsubo, K.: 30-year changes in the nitrogen inputs to the Yangtze River Basin, Environ. Res. Lett., 9, 115005, doi:10.1088/1748-9326/9/11/115005, 2014.

Ye, F., Huang, X., Zhang, X., Zhang, D., Zeng, Y., and Tian, L.: Recent oxygen depletion in the Pearl River Estuary, South China: geochemical and microfaunal evidence, J. Oceanogr., 68, 387-400, doi:10.1007/s10872-012-0104-1, 2012.

Yu, F., Zong, Y., Lloyd, J. M., Huang, G., Leng, M. J., Kendrick, C., Lamb, A. L., and Yim, W. W.-S.: Bulk organic $\delta^{13}C$ and C/N as indicators for sediment sources in the Pearl River delta and estuary, southern China, Estuar. Coast. Shelf Sci., 87, 618-630, doi:10.1016/j.ecss.2010.02.018, 2010.

Zhang, J., Zhang, Z. F., Liu, S. M., Wu, Y., Xiong, H., and Chen, H. T.: Human impacts on the large world rivers: Would the Changjiang (Yangtze River) be an illustration?, Global Biogeochem. Cycles, 13, 1099-1105, doi:10.1029/1999GB900044, 1999.

Zhang, J., Cowie, G., and Naqvi, S. W. A.: Hypoxia in the changing marine environment, Environ. Res. Lett., 8, 015025, doi:10.1088/1748-9326/8/1/015025, 2013.

Zhang, Y., Xiao, W., and Jiao, N.: Linking biochemical properties of particles to particle-attached and free-living bacterial community structure along the particle density gradient from freshwater to open ocean, J. Geophys. Res. Biogeosci., 121, 2261-2274, doi:10.1002/2016JG003390, 2016.

Zhu, C., Wagner, T., Pan, J.-M., and Pancost, R. D.: Multiple sources and extensive degradation of terrestrial sedimentary organic matter across an energetic, wide continental shelf, Geochem. Geophys. Geosyst., 12, Q08011, doi:10.1029/2011GC003506, 2011.

Zimmerman, A. R. and Canuel, E. A.: A geochemical record of eutrophication and anoxia in Chesapeake Bay sediments: anthropogenic influence on organic matter composition, Mar. Chem., 69, 117-137, doi:10.1016/S0304-4203(99)00100-0, 2000.

Biogeosciences Discuss., doi:10.5194/bg-2017-43, 2017
Manuscript under review for journal Biogeosciences
Discussion started: 22 February 2017

Table 1. Summary of the end-member values and their uncertainties adopted in the three end-member mixing model.

Water Mass	θ(°C)	Salinity	DIC (μmol kg^{-1})	$\delta^{13}C_{DIC}$ (‰)	Ca^{2+} (μmol kg^{-1})
Plume	30.6±1.0	10.8	1670±50[a]	-7.0[b]	3620[c]
Surface	31.0±1.0	33.7±0.2	1917±3	0.6±0.2	9778[c]
Subsurface	21.8±1.0	34.6±0.1	2023±6	0.1±0.1	10053

[a] In order to derive a proper plume end-member value, we took advantage of a 3 years' surface dataset in summer cruises (see Sect. 4.1). For DIC, the data is from cruises in August 2012, July 2014 and July 2015.

[b] The $\delta^{13}C_{DIC}$ value was 0.6±0.2 ‰ in the off-shore surface seawater at S=~33.7, and -11.4±0.2 ‰ at S<0.4 near the freshwater source in this cruise. Assuming the plume water is a mixture between freshwater and the off-shore surface seawater, the $\delta^{13}C_{DIC}$ of plume water end-member (S=10.8) can be calculated via the isotope mass balance, which equals -7.0 ‰.

[c] The Ca^{2+} values of the plume and surface seawater EM are derived from a conservative mixing calculation (Ca^{2+} vs. S) based on the cruise data in August 2012.

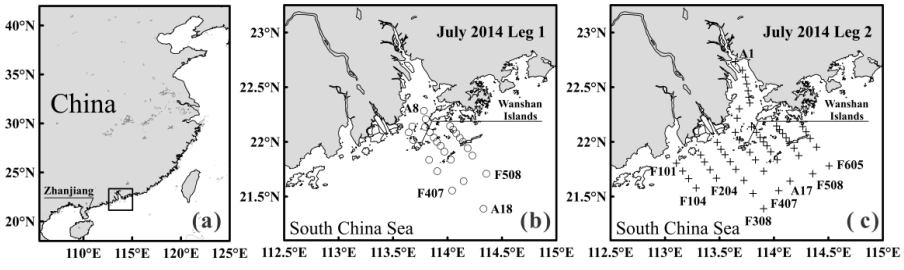

Figure 1. Map of the Pearl River Estuary and the adjacent coastal water (a). The open circles denote the Leg 1 stations on 13–16 July 2014 (b) and the crosses represent the Leg 2 stations on 19–27 July 2014 (c).

Biogeosciences Discuss., doi:10.5194/bg-2017-43, 2017
Manuscript under review for journal Biogeosciences
Discussion started: 22 February 2017

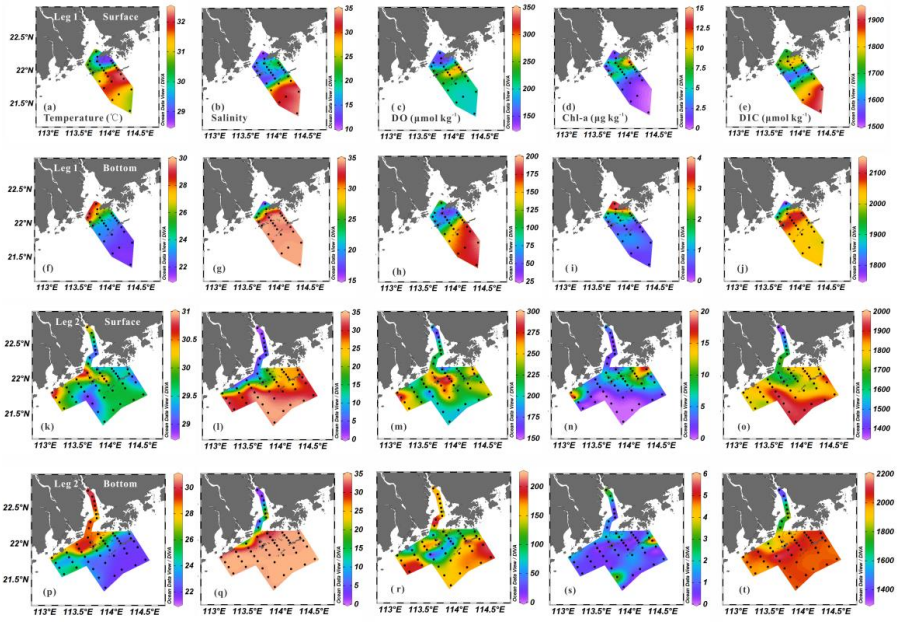

Figure 2. Surface and bottom distributions of temperature, salinity, DO, Chl-a and DIC belonging to Leg 1 (a–e, f–j) and Leg 2 (k–o, p–t).

Biogeosciences Discuss., doi:10.5194/bg-2017-43, 2017
Manuscript under review for journal Biogeosciences
Discussion started: 22 February 2017

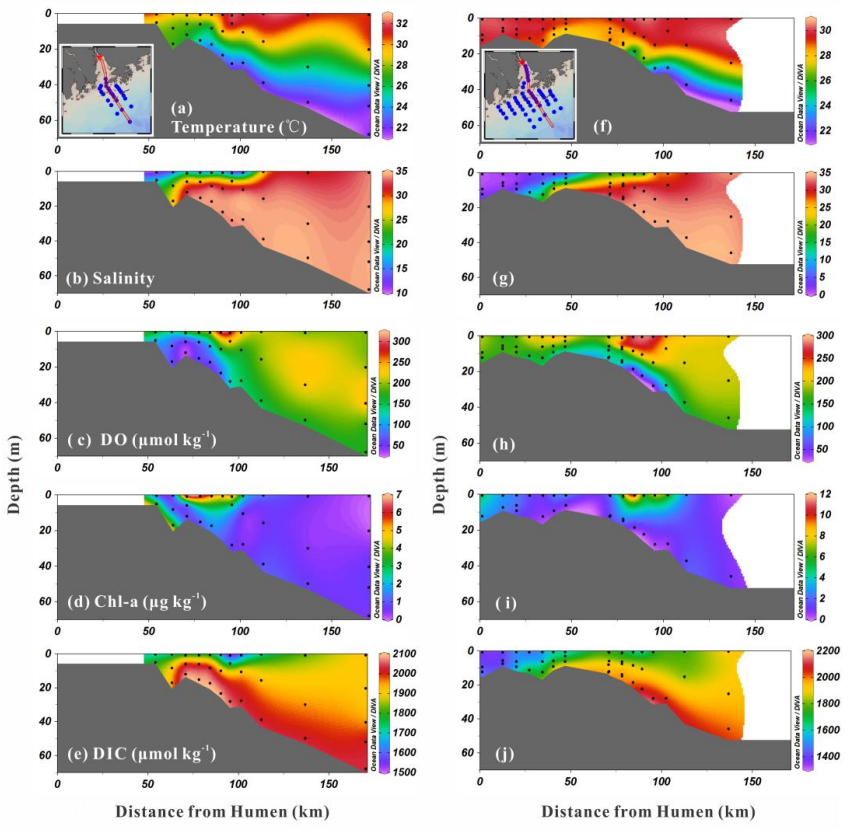

Figure 3. Profiles of temperature, salinity, DO, Chl-a and DIC along Transect A in Leg 1 (a–e) and Leg 2 (f–j).

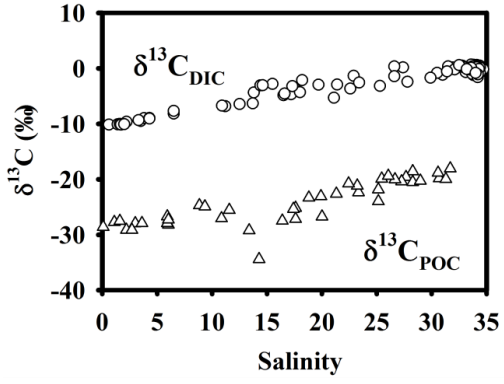

Figure 4. Distribution of $\delta^{13}C_{DIC}$ and $\delta^{13}C_{POC}$ along with salinity in the PRE and the adjacent coastal water. The open circles denote the $\delta^{13}C_{DIC}$ data in July 2014, while the open triangles represent the $\delta^{13}C_{POC}$ in July 2015.

Biogeosciences Discuss., doi:10.5194/bg-2017-43, 2017
Manuscript under review for journal Biogeosciences
Discussion started: 22 February 2017

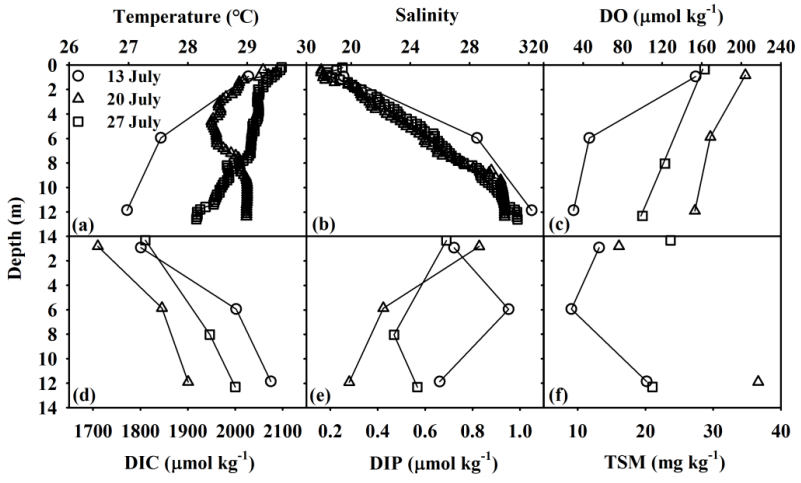

Figure 5. Profiles of (a) temperature, (b) salinity, (c) DO, (d) DIC, (e) DIP, (f) TSM and their evolution during repeated sampling at Station A10.

Biogeosciences Discuss., doi:10.5194/bg-2017-43, 2017
Manuscript under review for journal Biogeosciences
Discussion started: 22 February 2017

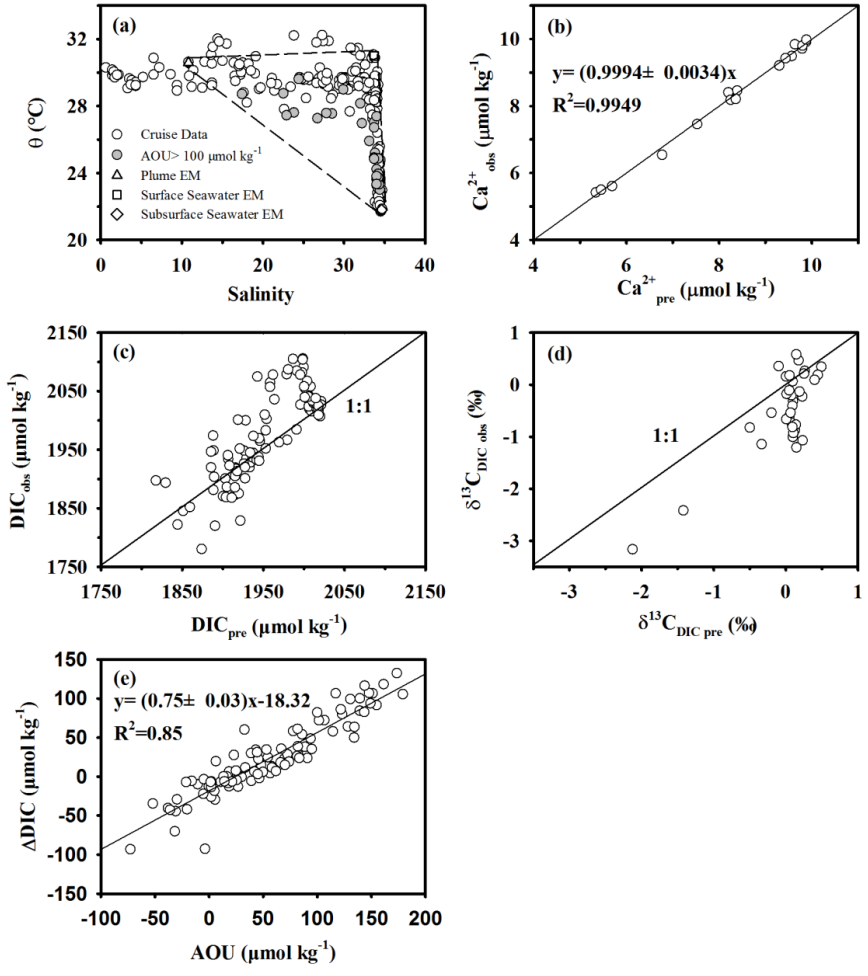

Figure 6. (a) The potential temperature (θ) (℃) vs. salinity scheme in the PRE and adjacent coastal water (open circles) based on the data collected in the July 2014 cruise. The grey filled circles show the low oxygen sites, where AOU> 100 μmol kg^{-1}. The three end-members, including plume water (open triangle), off-shore surface seawater (open square) and subsurface seawater (open diamond) are also displayed; (b) Relationships between the field-observed Ca^{2+} (Ca^{2+}_{obs}) and model-predicted Ca^{2+} (Ca^{2+}_{pre}). The straight line denotes a linear regression line; (c), (d) Relationships between the observed DIC, $\delta^{13}C_{DIC}$ and model-predicted DIC, $\delta^{13}C_{DIC}$. The straight lines act as a 1:1 reference line; and (e) Relationships of ΔDIC vs. AOU for all the data belonging to the subsurface water. ΔDIC is the difference between the field-observed DIC and model-predicted DIC.

Biogeosciences Discuss., doi:10.5194/bg-2017-43, 2017
Manuscript under review for journal Biogeosciences
Discussion started: 22 February 2017

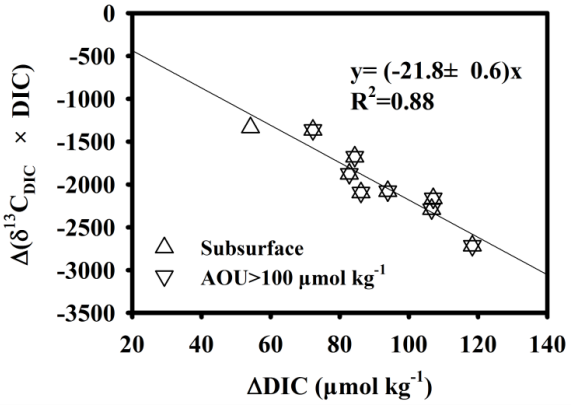

Figure 7. Plot of Δ ($\delta^{13}C_{DIC}\times$DIC) vs. ΔDIC for samples collected in the subsurface water (>5 m, up triangles). The down triangles represent the samples with AOU > 100 µmol kg^{-1}. Δ is the difference between the field-observed and model-predicted values.

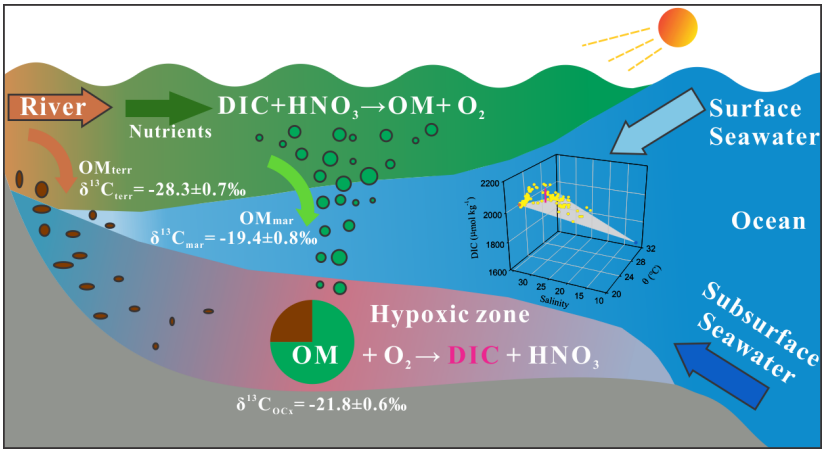

Figure 8. A conceptual diagram illustrating the source partitioning of oxygen-consuming organic matter (OC_{mar} vs. OC_{terr}) within the hypoxic zone in the lower PRE and the adjacent coastal area. See Sect. 4.2 for explanations.